ELSEVIER

Optics & Laser Technology 31 (1999) 141–149

Optics & Laser Technology

www.elsevier.com/locate/optlastec

Effects of image compression on PIV and PTV analysis

A. Cenedese[a,*], A. Pocecco[b], G. Querzoli[b]

[a]Dipartimento di Idraulica, Trasporti e Strade, Università di Roma 'La Sapienza', Rome, Italy
[b]Dipartimento di Ingegneria Civile, Università di Roma 'Tor Vergata', Rome, Italy

Received 20 July 1998; received in revised form 19 February 1999; accepted 19 February 1999

Abstract

PIV and PTV analysis require the acquisition of series of images, representing the position of seeding particles at different times, resulting in a great amount of data to be stored on magnetic support, such as hard disk and magnetic tape. Typical dimensions of a PIV image are 1000×1000 pixels which results in 1 Mb per image (grey levels) to be stored. In this work the capabilities of different methods for data compression are evaluated and their effects on PIV and PTV analysis are compared.

1. Introduction

It is well known that increasing image resolution and frame rate together will improve PIV or PTV measurements. Unfortunately this results in a huge amount of information to be stored during acquisition. For example, to digitize 256 grey levels images at the standard PAL resolution (752×576 pixels) and rate (25 frames per second) it is necessary to have a transfer rate of about 10 MB per second. At present this is not compatible with a standard storage device both because of their transfer rate and of their total capacity. This problem is even more serious when dealing with the high resolution cameras (up to 2048×2048 pixels) and/or fast cameras (up to 2000 frames per second) that have been recently developed.

Digital images acquired for PIV and PTV, in their canonical representation, generally contain a large amount of redundancy and it is possible to take advantage of this redundancy to reduce the number of bits required to represent an image. This leads to significant savings in the memory needed for the image storage thus reducing both the required transfer rate and total capacity of devices.

The approaches to image compression can be categorized into two fundamental groups: lossless and lossy.

In lossless compression (or reversible compression), the memory saving in the image representation is obtained without any loss of information. This means that, once compressed, the original image can be exactly reconstructed by reverting the compression procedure.

In lossy compression (or irreversible compression), the reconstructed image contains degradation relative to the original. The aim of lossy techniques is to reduce the amount of memory needs by excluding those parts of the information that are not useful to the ensuing analysis. As a result, even if lossless compression is ideally desired, the lossy one is often chosen because much higher compression can be achieved and procedures are faster: obviously, the time required to perform image compression is a crucial parameter when acquiring series of images.

Apparently, the concept of what is useful and what is not among the information contained in an image depends on what is represented on the images and on the aim for which the image is acquired. A series of tests have been performed to determine how much it is possible to compress a PIV (or a PTV) image without a significant loss of information on the velocity field.

* Corresponding author. Tel.: +39-6-4458-5033; fax: +39-6-4458-5217.

E-mail address: icola@cenedese1.ing.uniromal.it (A. Cenedese)

0030-3992/99/$ - see front matter
PII: S0030-3992(99)00018-3

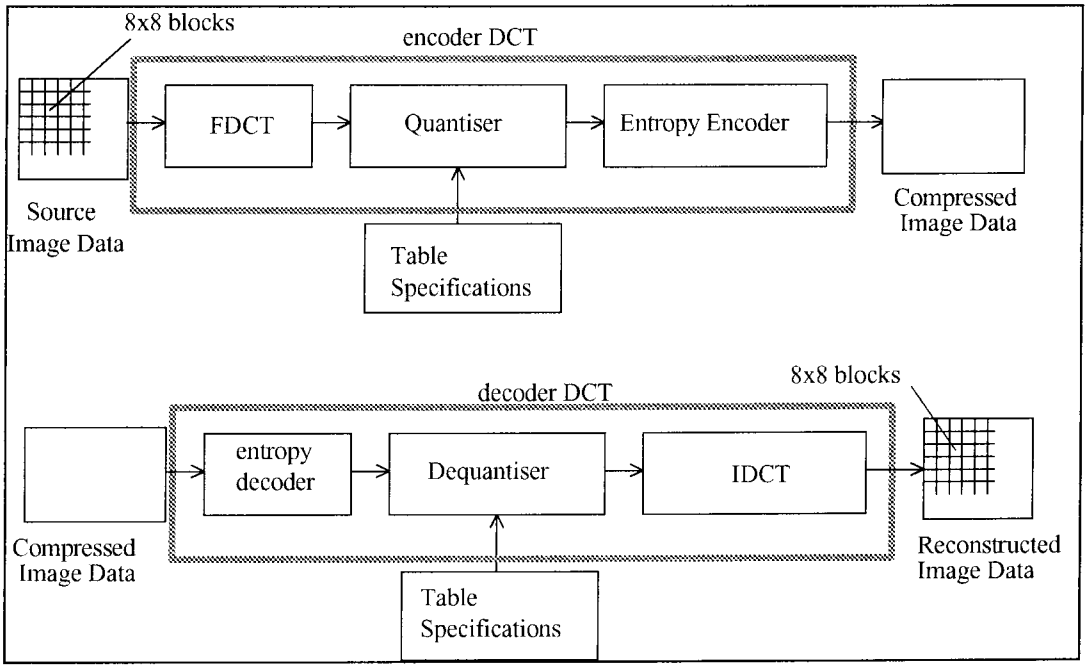

Fig. 1. JPEG compression scheme.

2. The compression process

2.1. General

Fig. 1 shows the fundamental steps of data compression carried out by JPEG encoding [1, 2]. At the input to the encoder source image samples are grouped into 8×8 blocks and then processed. The encoder is considered to be divided into three main blocks:

- FDCT (fast discrete cosine transform)

$$F(u, v) = \tfrac{1}{4}C(u)C(v)\left[\sum_{x=0}^{7}\sum_{y=0}^{7} f(x, y) \times \cos\frac{(2x+1)u\pi}{16}\cos\frac{(2y+1)v\pi}{16}\right],$$

  where $C(u)$, $C(v) = 1/\sqrt{2}$ for u, $v = 0$; $C(u)$, $C(v) = 1$ otherwise.
- Quantizer, the element where the selection on data spectral content takes place.
- Entropy encoder, where data are appropriately encoded using their statistical characteristics.

In Fig. 1, the JPEG decoder, that reverses these processing steps and reconstructs the image, is also sketched.

2.2. Transformation

DCT (discrete cosine transform) [3], has a higher compression efficiency than DFT (discrete Fourier transform), since it does not generate spurious spectral

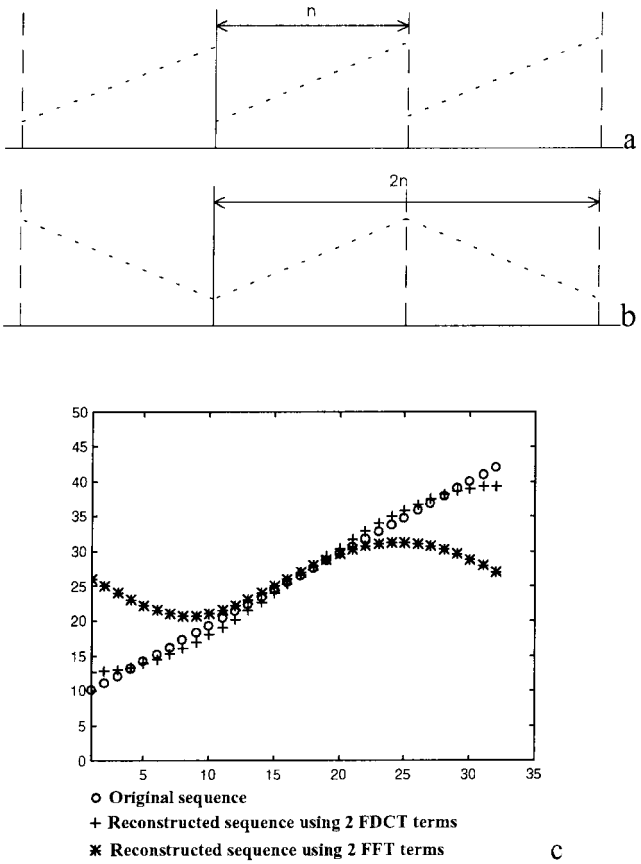

Fig. 2. Original and $2n$-points extended sequences.

Table 1
Example of JPEG encoding and decoding procedure

(a) Source image samples

139	144	149	153	155	155	155	155
144	151	153	156	159	156	156	156
150	155	160	163	158	156	156	156
159	161	162	160	160	159	159	159
159	160	161	162	155	155	155	155
161	161	161	161	160	157	157	157
162	162	161	163	162	157	157	157
162	162	161	161	163	158	158	158

(b) Forward DCT coefficient

235.6	−1.0	−12.1	−5.2	2.1	−1.7	−2.7	1.3
−22.6	−17.5	−6.2	−3.2	−2.9	−0.1	0.4	−1.2
−10.9	−9.3	−1.6	1.5	0.2	−0.9	−0.6	−0.1
−7.1	−1.9	0.2	1.5	0.9	−0.1	0.0	0.3
−0.6	−0.8	1.5	1.6	−0.1	−0.7	0.6	1.3
1.8	−0.2	1.6	−0.3	−0.8	1.5	1.0	−1.0
−1.3	−0.4	−0.3	−1.5	−0.5	1.7	1.1	−0.8
−2.6	1.6	−3.8	−1.8	1.9	1.2	−0.6	−0.4

(c) quantization table

16	11	10	16	24	40	51	61
12	12	14	19	26	58	60	55
14	13	16	24	40	57	69	56
14	17	22	29	51	87	80	62
18	22	37	56	68	109	103	77
24	35	55	64	81	104	113	92
49	64	78	87	103	121	120	101
72	92	95	98	112	100	103	99

(d) normalized quantized coefficients

15.	0	−1	0	0	0	0	0
−2	−1	0	0	0	0	0	0
−1	−1	0	0	0	0	0	0
0	0	0	0	0	0	0	0
0	0	0	0	0	0	0	0
0	0	0	0	0	0	0	0
0	0	0	0	0	0	0	0
0	0	0	0	0	0	0	0

(e) denormalized quantized coefficients

240	0	−10	0	0	0	0	0
−24	−12	0	0	0	0	0	0
−14	−13	0	0	0	0	0	0
0	0	0	0	0	0	0	0
0	0	0	0	0	0	0	0
0	0	0	0	0	0	0	0
0	0	0	0	0	0	0	0
0	0	0	0	0	0	0	0

(f) reconstructed image samples

144	146	149	152	154	156	156	156
148	150	152	154	156	156	156	156
155	156	157	158	158	157	156	155
160	161	161	162	161	159	157	155
163	163	164	163	162	160	158	156
163	164	164	164	162	160	158	157
160	16	162	162	162	161	159	158
158	159	161	161	162	161	159	158

components. There is an implicit periodicity of the original samples sequence, using DFT, that is the result of sampling in the frequency domain (Fig. 2(a)). This periodicity often creates severe discontinuities which cause, for their representation, spurious high frequency components. A possible method of eliminating such discontinuities, is to extend the original n-point sequence to a $2n$-point one. As shown in Fig. 2(b) this periodic sequence does not have any discontinuity. Taking a $2n$-point DFT extended sequence is identical to the DCT of the original n-point sequence. As shown in Fig. 2(c) more DFT than DCT coefficients are needed to represent correctly the original sample sequence. This is a major advantage of DCT over DFT, besides DCT is more efficient since it requires only real computations [4].

Each block of source image samples can be considered as a 64-point discrete signal which is a function of the two spatial coordinates x and y. The FDCT decomposes such a signal into 64 orthogonal basis signals, each one representing a two-dimensional 'spatial frequency'. The compression process lays its foundation in concentrating most of the signal in the lower spatial frequencies, neglecting the others through the so called quantization process. The decoder reverses this processing steps and reconstructs the image by summing the basis signals.

2.3. Quantization

The quantization process is based essentially on the determination of particular coefficients represented as 8×8 matrices that determine the 'weight' to give to each spatial frequencies. Quantization, $F^Q(u, v)$, is defined as the division of each DCT coefficient F, by its corresponding quantizer step size Q and then rounding to the nearest integer:

$$F^Q(u, v) = \mathrm{int}\left(\frac{F(u, v)}{Q(u, v)}\right). \tag{1}$$

Dequantization is the inverse operation, performed by multiplying the quantized coefficients by the step size:

$$F^{Q\prime}(u, v) = F^Q(u, v)Q(u, v). \tag{2}$$

2.4. Entropy encoding

The quantized coefficients must be Huffman-

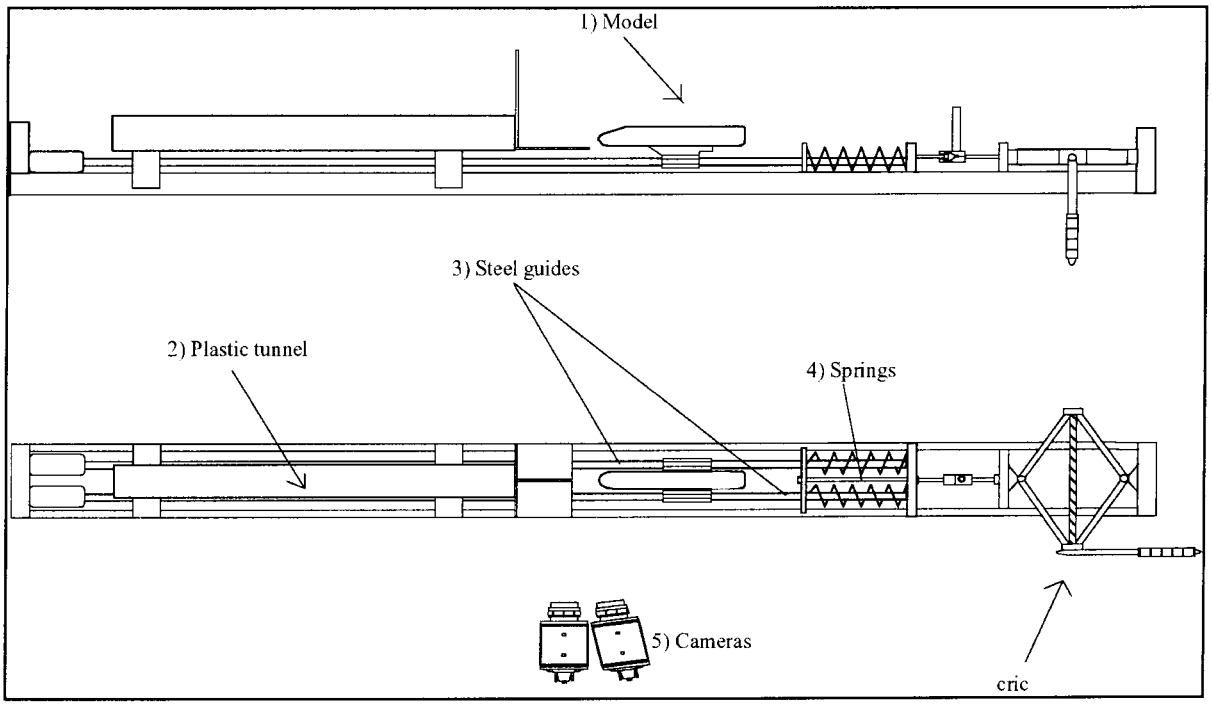

Fig. 3. The mechanical equipment: (1) The model representing the train profile. (2) The tunnel made in perspex. (3) Two steel rods which guide the model into the tunnel. (4) Two springs to launch the model. (5) Two high resolution digital cameras equipped with narrow-band filters in order to allow only one laser wavelength to reach the CCD.

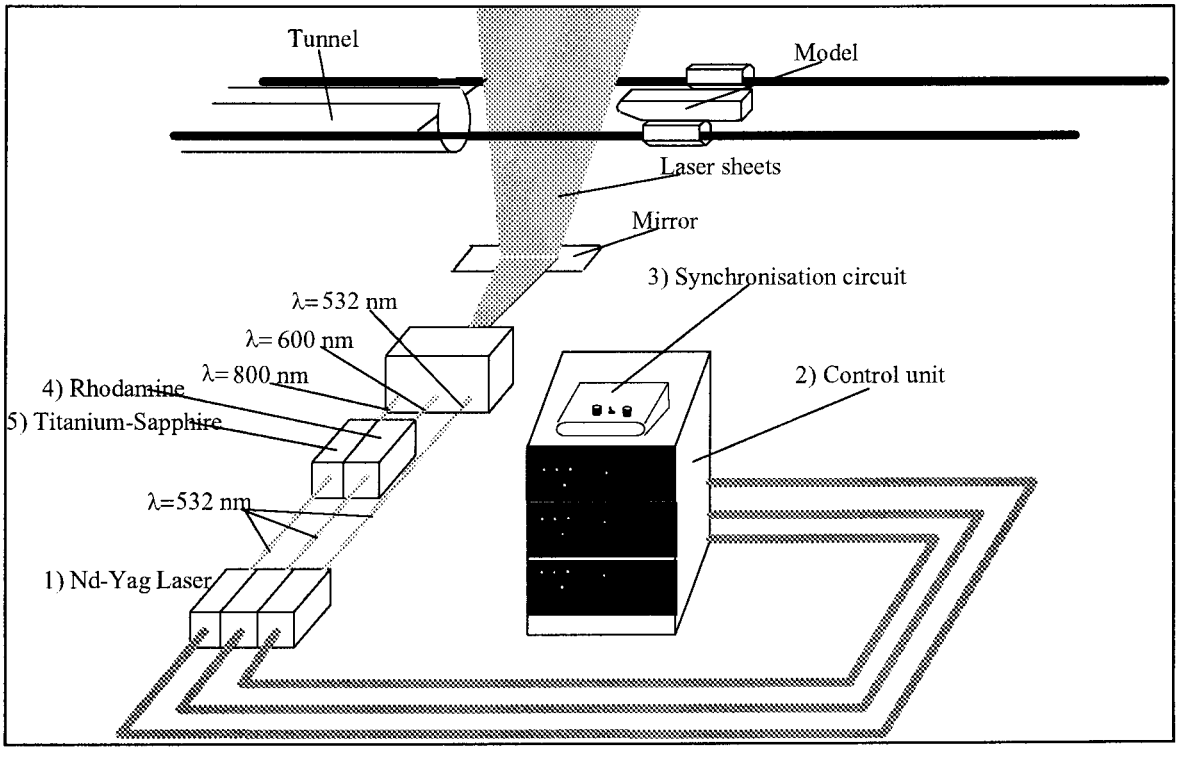

Fig. 4. The laser equipment. (1) Three Nd–Yag lasers emitting laser pulses with a frequency equal to 10 Hz. (2) The laser control unit which allows the regulation of the power and the delay of the laser pulses. (3) The circuit which allows the synchronization of the image acquisition with the position of the model. (4) Rhodamine diluted with alcohol changes the Nd–Yag laser wavelength to 600 nm. (5) A titanium–sapphire crystal changes the Nd–Yag laser wavelength to 800 nm.

encoded, since there are usually many zero coefficients after quantization [5]. The aim of Huffman coding is to represent these coefficients efficiently. They are converted into an intermediate sequence of symbols where variable length codes are assigned to the symbols and then encoded following a zig-zag scheme. Table 1 shows an example of JPEG encoding and decoding procedures on a 8×8 matrix representing a portion of an image.

Table 2
File dimensions for different compression levels

JPEG compression level	Bytes
0	1,049,654
25	392,592
50	265,898
75	172,187
99	36,357
Lossless compression	857,506

3. Experimental set-up

3.1. Types of image

Images for velocimetry can be divided into two main categories: multi-exposed images and single exposed ones. While the first category permits an easier study of phenomena with rather simple experimental methodology, the second one provides a richer information, reducing ambiguities in the identification of particle displacements and resolving the velocity sign. This latter is a fundamental feature in the study of complicated flow fields, especially where the overall behavior of the velocities is not known a priori. Another important advantage of single-exposed image analysis is the dynamic range of measurement. To obtain a good description in areas characterized by high velocities the time interval between the laser pulses must be short. In low velocity areas, however,

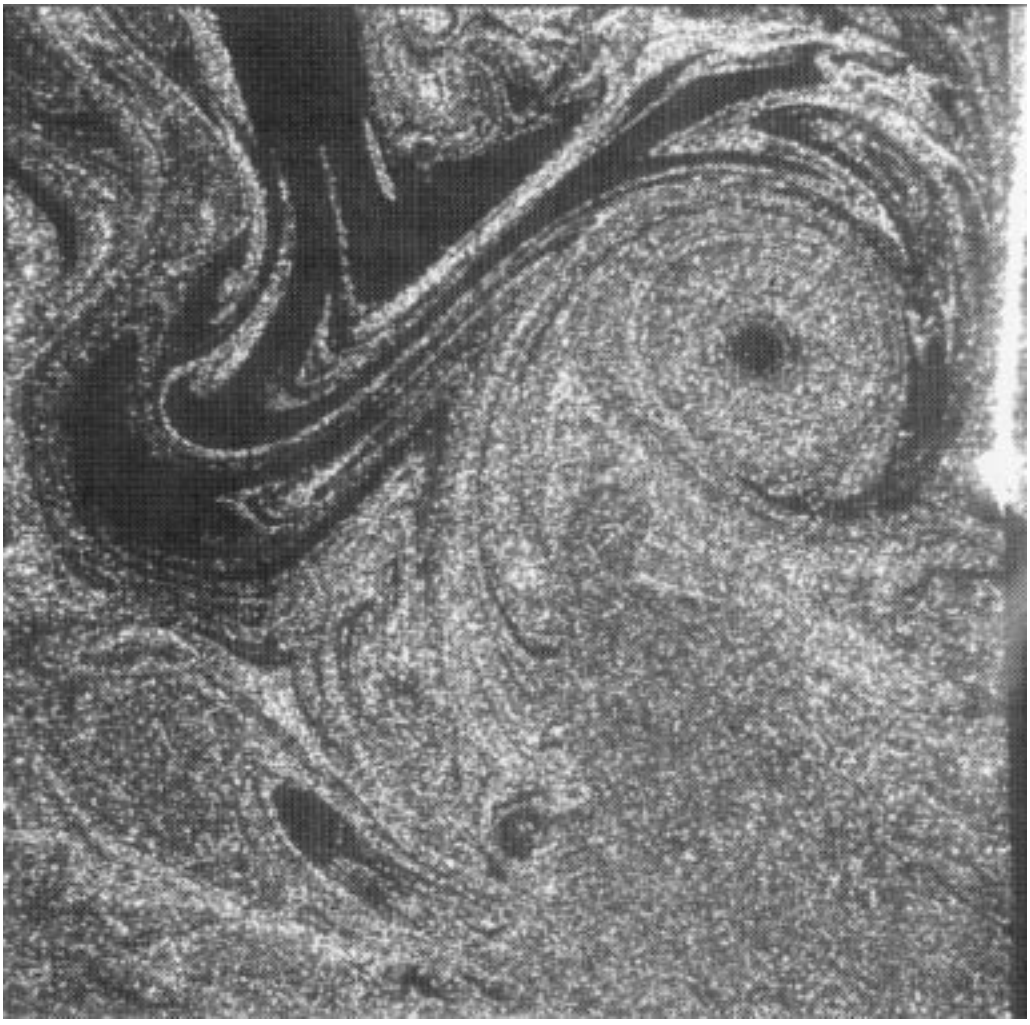

Fig. 5. Original image.

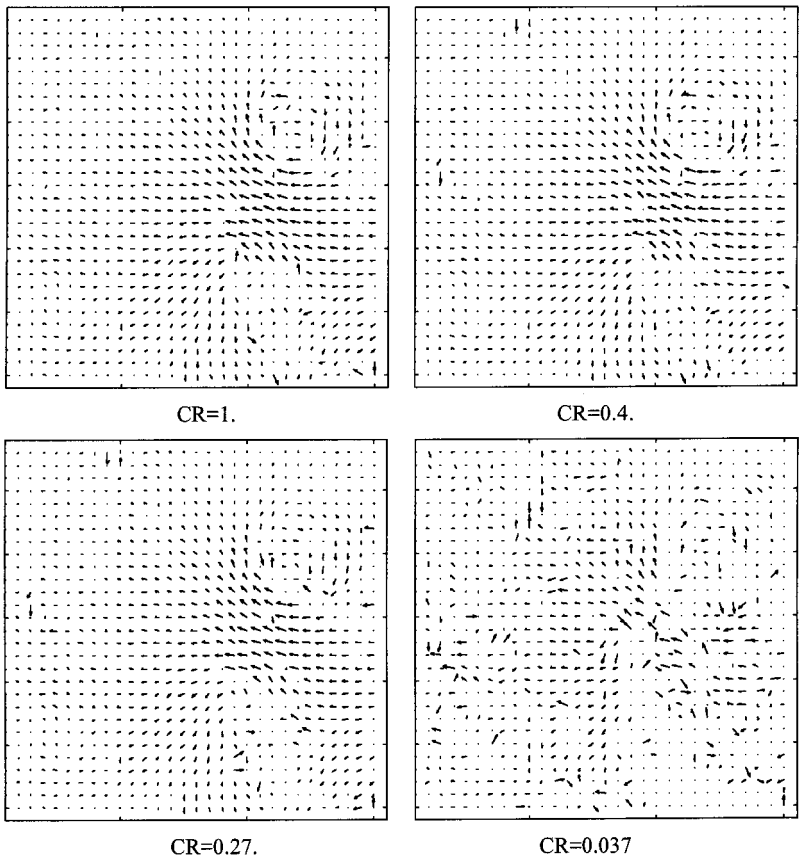

Fig. 6. Velocity fields at different compression levels.

short time intervals can result the superimposition of particle images resulting in a loss of information [6, 7].

3.2. Experimental equipment

The PIV test experiment is a laboratory simulation of a train entering a tunnel, whose main components are:

- Mechanical equipment for the model (Fig. 3).
- An Nd–Yag laser (Fig. 4) emitting at three wavelengths with the following energy levels: 532 nm 100 mJ, 600 nm 50 mJ and 800 nm 50 mJ.
- Two high resolution cameras (2048 × 2048 pixels).
- A workstation equipped with cards for image acquisition.
- An electronic device for laser synchronization.

The air in the proximity of the tunnel was seeded with small olive oil particles. They were illuminated by a light sheet created by the laser generating two colored pulses. Pairs of high resolution images were acquired by the two aligned high resolution cameras. Each camera was equipped with a narrow-band filter centered on the wave-length of one of the pulses and the velocity field was evaluated through a cross-correlation technique.

4. PIV from compressed images

The size of the acquired images are 2048 × 2048 so, the space occupied on disk is nearly 4 MB; for PIV analysis two or three images are needed for each elaboration, so it is apparent that a great amount of data needs to be recorded on magnetic supports. For these reasons the image files were compressed, using the JPEG compression procedure of Fig. 1. Table 2 shows, as an example, the amount of memory required at

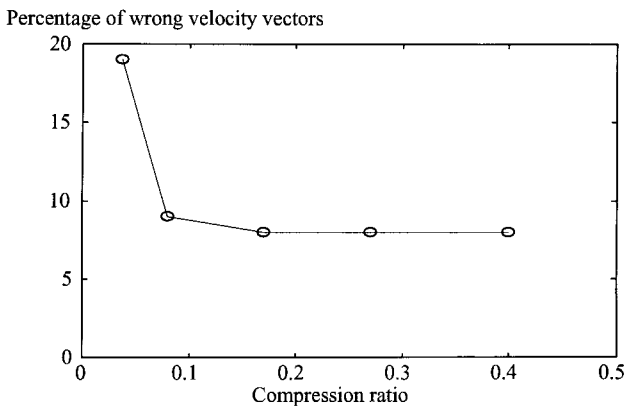

Fig. 7. Effects of lossy compression procedure on velocity field.

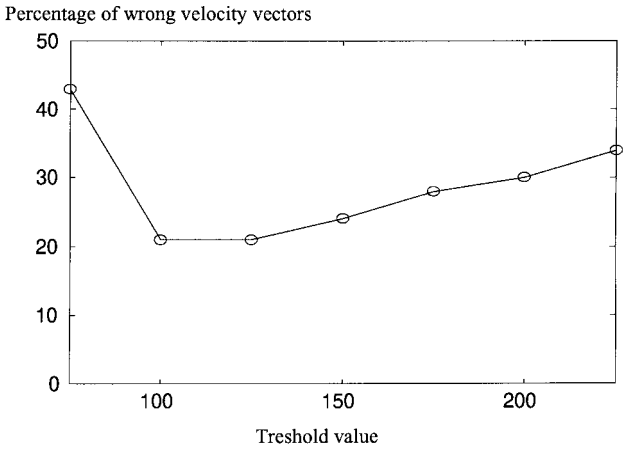

Fig. 8. Effects of lossless compression procedure on velocity field.

different JPEG compression level for a 1024×1024 image; the last line shows the result of a lossless compression technique and can be considered representative of the amount of information contained in the image.

The image shown in Fig. 5 was compressed at different levels and then analyzed, after decompression, using a cross-correlation technique to evaluate the effect of image compression on the reconstruction of a fluid flow. Fig. 6 shows the velocity vector fields obtained for different values of compression ratio (CR) where:

$$\mathrm{CR} = \frac{\text{numbers of bits for compressed image}}{\text{numbers of bits for original image}}.$$

Fig. 7 shows the effects of image compression by representing the errors detected as a function of compression ratio. As described previously, JPEG is a lossy technique so, by increasing the compression level the image quality decreases. This leads to corresponding corruption in the image resulting, in many cases, in the erroneous detection of the main correlation peak, due to the predominance of noise. The curve plotted exhibits a sharp increase in errors for CR lower than 0.1, whereas it is almost flat for larger CR values. This means that the number of errors does not increase significantly when compressing the image down to $\mathrm{CR} = 0.1$ which seems to be, for the present data-set, the optimal compression rate.

5. An alternative compression method for PIV images

In the general attempt to reduce the amount of space required to memorize the image files, another method was evaluated. As a first step a *threshold* value was chosen to decrease the number of grey levels from 256 to 2. The two-dimensional luminance function of the image was reduced by assuming the value of 0 or 255 if its local value is lesser or greater than the threshold level chosen. The number of bits required to store this file has now been reduced from 8 to 1 ($\mathrm{CR} = 0.125$). As a consequence, it has been possible to compress a 1024×1024 image from 1,049,000 bytes to 131,125 bytes. The resulting image is further compressed to 84,000 ($\mathrm{CR} = 0.08$) using a lossless technique.

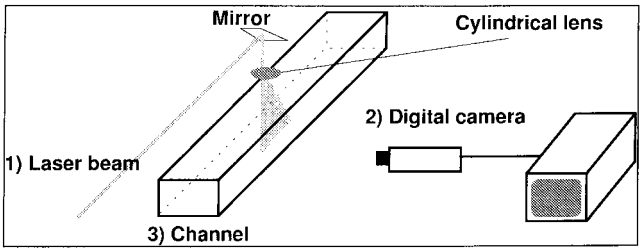

Fig. 9. Experimental set-up for PTV analysis. (1) The laser beam (Argon) is made into a sheet by using a cylindrical lens. (2) A digital camera allows the acquisition of image sequences for PTV analysis. (3) A channel made in perspex to achieve a one-dimensional flow.

From the assessment of the percentage error (Fig. 8) as a function of threshold value, it is apparent that the optimum value for this case, is 125, corresponding to a percentage of wrong velocity vectors of nearly 20. If however the JPEG technique is used, with the same compression ratio (Fig. 7), the percentage of errors is only 8, hence it is clear that the JPEG procedure gives better results.

6. PTV from compressed images

In order to test the effects of compression on images acquired using particle tracking velocimetry (PTV) [8], tests have been performed on images representing a near wall flow. The experimental set-up is represented in Fig. 9. It is composed of:

- a channel made in perspex,
- a high speed camera able to acquire up to 2000 frame/s and equipped with a CCD sensor whose active area is 480×420 pixels,
- an Ar–Ion. laser beam (1 W) giving a sheet illumination of the test section by means of a cylindrical lens and
- metal-coated particles (4 μm diameter) are used as seeding.

Fig. 10(a) shows three superimposed, single exposed images recorded at 50 frame/s. The image sequence was used to identify the particle trajectories and to evaluate the effects of image compression. The images were compressed at different levels and the results of tracking were compared.

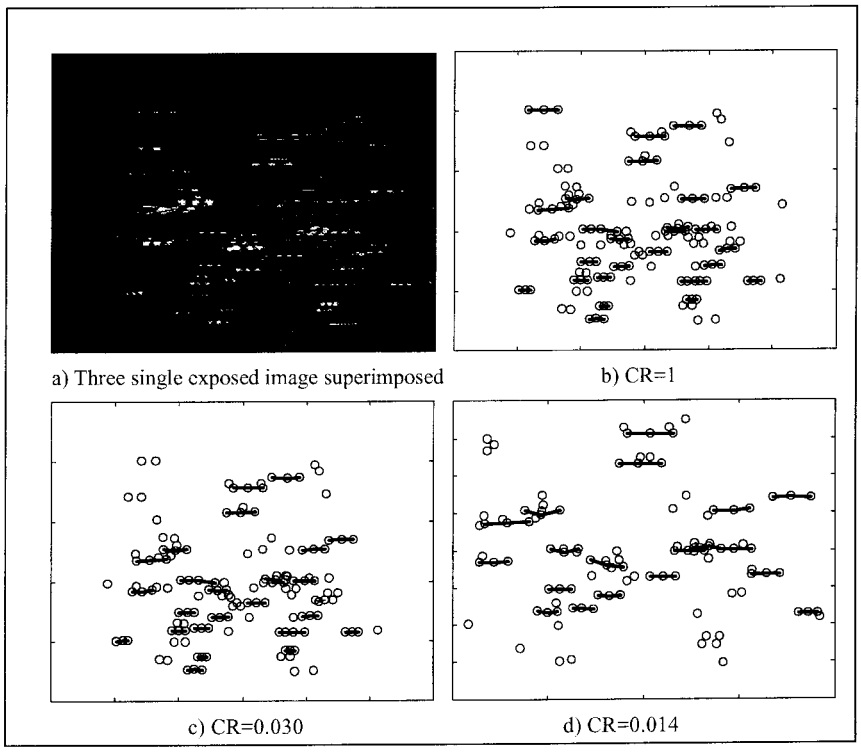

Fig. 10. Recognized trajectories.

The PTV process consists of four basic steps:

- image acquisition
- thresholding
- particle centroid identification
- trajectory recognition

A first test was carried out on the acquired images by compressing them at different JPEG levels. Then the analysis was conducted using the same tracking parameters and comparing the results in terms of identification of trajectories for different values of CR (Fig. 10(b–d)). Fig. 11 gives the number of identified

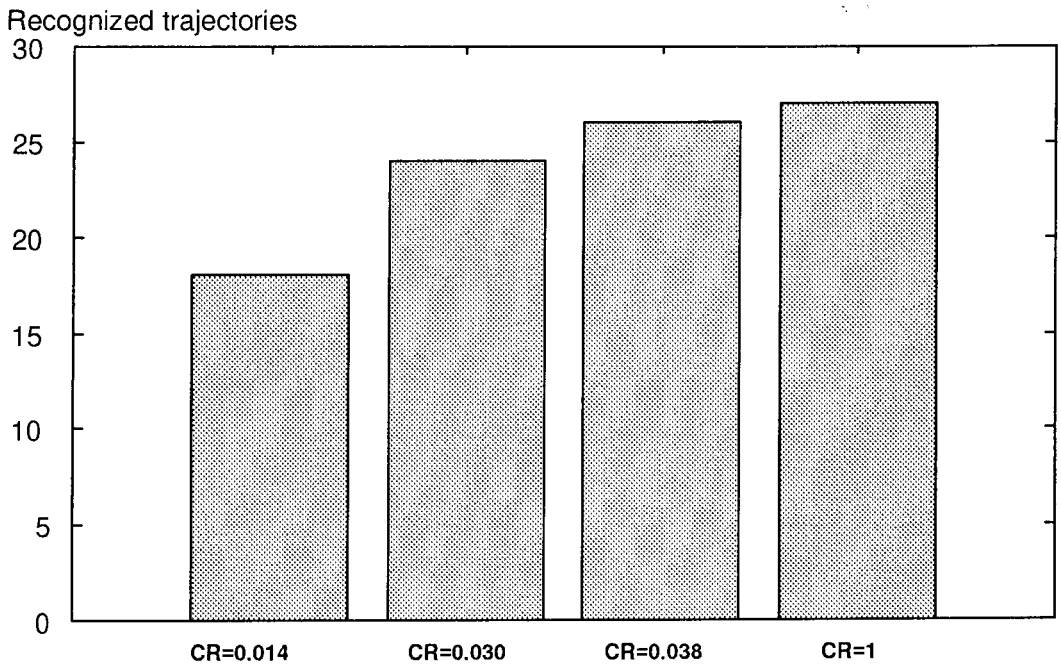

Fig. 11. Number of recognized trajectories versus CR.

trajectories as a function of compression ratio (CR); it is evident that high compression levels cause significant loss of information due to severe corruption of the particle images. On the other hand, it should be noted that PTV images differ from those from PIV for one main reason: the seeding density is usually much lower so, large areas of a PTV image merely represent the background and are black or uniformly very dark. This characteristic suggests that high compression levels can be reached by using a *lossless* compression technique on the thresholded image, as described in Section 1. When applied to the present image this procedure could tolerate a CR as low as 0.0035 without loss of velocity information. The result suggests that lossless compression of thresholded images is a more effective technique when storing PTV images.

7. Conclusions

The performance of techniques requiring image analysis, namely PIV and PTV, is chiefly affected by two parameters: image resolution and the frame rate. Increasing these parameters however is limited by the large amount of data needed to represent digital images which results also in a massive transfer rate to the storage devices, such as hard discs. This technological constraint may be overcome by reducing the number of bits used to represent images via a compression method. Such an operation would reduce both the data transfer rate and the total amount of space required by the images. In this paper lossy and lossless compression techniques have been tested both on PIV and PTV images. PIV images are usually characterized by a high seeding density so a lossless compression is not very effective. However PIV image processing coupled with lossy compression has been successfully carried out here even if some details of the images have not been preserved. Hence we conclude that high levels of compression may be employed with a lossy technique such as JPEG without significant degradation of the resulting velocity fields.

In contrast to PIV, PTV is based on the identification of single particle images. As a consequence, the loss of even a few image details can seriously affect the results. Further, PTV images often exhibit a low seeding density and large areas are uniformly black. We have found for these images that lossless compression is quite effective. In addition the most important characteristic for a successful compression of PTV images is that they are thresholded prior to further processing. Boolean images can be losslessy compressed much better than grey level ones, because more than 99% of the pixels are usually set to zero in a PTV, thresholded image. All these considerations allow us to conclude from this initial study that the best way to treat PTV kinds of images is via lossless compression after thresholding.

Acknowledgements

This work has been performed under the EUROPIV project. EUROPIV (a cooperative action to apply particle image velocimetry to problems of industrial interest) is a collaboration between LML URA CNRS 1441, DASSAULT AVIATION, DASA, SIREHNA, CIRA, DLR, DRA, FFA, INTA, ISL, NLR, ONERA, VKI and the universities of Delft, Madrid, Oldenburg, Rome, Rouen (CORIA URA CNRS 230), St Etienne (TSI URA CNRS 842), Warwick. The project is managed by LML URA CNRS 1441 and is funded by the CEC under the IMT initiative (contract No.: BR.PR-CT95-0118).

References

1 Wallace GK. The JPEG compression standard. IEEE Transaction on Consumer Electronic, 1991.
2 Léger A, Omachi T, Wallace G. The JPEG still picture compression algorithm. Optical Engineering 1991;30(7).
3 Rao KR, Yip P. Discrete cosine transform: algorithm, advantages, applications. Academic Press, 1990.
4 Rabbani M, Jones PW. Digital image compression technique. SPIE Optical Engineering Press, 1991.
5 Huffman DA. A method for the construction of minimum redundancy codes. In: Proceeding IRE, vol. 40, 1962.
6 Keane RD, Adrian RJ. Theory of cross-correlation analysis of PIV images. Applied Scientific Research 1992;49.
7 Cenedese A, Romano GP. PIV: a new technique in flow velocity mesurement. Excerpta of the Italian Hydraulic Society, 1990.
8 Querzoli G. Lagrangian and Eulerian description of turbolence in the unstable atmospheric boundary layer. Excerpta of the Italian Hydraulic Society, 1995.